[CANCER RESEARCH 62, 4229–4235, August 1, 2002]

Trapping of DNA Nucleotide Excision Repair Factors by Nonrepairable Carcinogen Adducts[1]

Tonko Buterin, Martin T. Hess, Daniela Gunz, Nicholas E. Geacintov, Leon H. Mullenders, and Hanspeter Naegeli[2]

Institute of Pharmacology and Toxicology, University of Zürich-Tierspital, CH-8008 Zürich, Switzerland [T. B., M. T. H., D. G., H. N.]; Chemistry Department, New York University, New York, New York 10003 [N. E. G.]; and Department of Radiation Genetics and Chemical Mutagenesis, Leiden University Medical Center, 2333 AL Leiden, the Netherlands [L. H. M.]

ABSTRACT

Nucleotide excision repair is part of a cellular defense system that protects genome integrity. Here, this versatile repair system was challenged with mixtures of DNA adducts that were generated to mimic the wide spectrum of bulky lesions produced by complex genotoxic insults. Probing human excision activity with substrate combinations instead of single lesions resulted in a strong bias for particular base adducts, such that the repair factors were immobilized on a small fraction of damaged DNA, whereas the simultaneous excision of other sites was suppressed. Immobilization of excision factors was also induced by nonrepairable decoy adducts, thereby revealing a mechanism of repair inhibition because of hijacking of critical subunits. Thus, the efficiency of excision repair in response to bulky carcinogen-DNA damage is dependent on an antagonistic interaction with both substrate and decoy adducts.

INTRODUCTION

To cope with bulky DNA damage induced by environmental carcinogens, all living organisms ranging from bacteria to humans are endowed with a versatile DNA repair system that removes many base defects (1–4). This universal repair reaction has been termed NER[3] because it operates through a cut and patch mechanism that is initiated by double endonucleolytic cleavage of phosphodiester bonds. One DNA incision occurs on the 3′ side to the lesion and the other on the 5′ side, thus releasing DNA damage as the component of single-stranded oligonucleotide segments (5). The excised nucleotides are replaced by DNA synthesis and ligation, thereby generating repair patches that, in human cells, extend over ~30 nucleotides in length (6).

All of the core NER subunits necessary for the removal of bulky DNA lesions in bacteria (7), yeast (8), and mammals (9–11) have been isolated and characterized. These repair factors lack specificity for a particular type of damage and, hence, recognize a nearly infinite range of base abnormalities. UV light, for example, generates two different types of covalent cross-links between adjacent bases, *i.e.*, CPDs and pyrimidine-pyrimidone (6-4) photoproducts, both of which are processed by the NER system (12–14). In view of this broad repair capacity, we analyzed the distribution of active human repair complexes between mixtures of chemically and structurally unrelated DNA lesions. Surprisingly, the combination of different standard substrates in human cell extracts showed that a minor fraction of damaged sites is able to monopolize a large proportion of NER complexes, whereas other concurrent lesions remain unrepaired. This finding provided a rational basis for engineering decoy adducts that are refractory to excision but nevertheless immobilize NER factors and compete for excision activity. The formation of such decoy adducts indicates that exposure to multiple DNA-damaging agents may result in hyper-additive genotoxic effects.

MATERIALS AND METHODS

DNA Substrates. A single AAF adduct at the C^8 position of guanine was generated by reacting the 19-mer oligonucleotide 5′-ACCACCCTTCGAACCACAC-3′ with *N*-acetoxy-AAF (15). A single platinum adduct at N^7 of guanine was obtained by incubating the same oligonucleotide (40 μM) with 400 μM of [Pt(dien)Cl]Cl (Ref. 16; generously provided by Dr. Giuseppe Villani, CNRS, Toulouse, France). Alternatively, this reaction was carried out with the 19-mer 5′-ACCACCCTTAGTACCACAC-3′, in which the central sequence 5′-CGA-3′ was replaced by 5′-AGT-3′. After incubations at 37°C for 18 h in 10 mM Tris-HCl (pH 8.0) and 1 mM EDTA, the platinum-damaged oligonucleotides were recovered by ethanol precipitation. Complete modification was verified by a reduced electrophoretic mobility of the adducted oligonucleotides. M13 double-stranded DNA (7287 bp) containing a site-directed lesion was constructed by ligating 19-mer oligonucleotides into a gapped circular DNA intermediate (17). Plasmids pSPORT (4110 bp; Life Technologies, Inc.) were irradiated (254 nm, 450 J/m^2) on ice in an open Petri dish in aliquots of 20 μl containing 35 nM DNA, 10 mM Tris-HCl (pH 8.0), and 1 mM EDTA. Subsequently, the DNA was incubated with *Escherichia coli* endonuclease III to remove plasmids that contain pyrimidine hydrates, and the residual closed circular substrate was separated from nicked DNA by 5–20% sucrose gradient centrifugation (18). Internally radiolabeled DNA fragments of 139 bp with a single base adduct in the center were constructed as described (19).

pUC19 Competitors. Plasmids pUC19 (2686 bp) containing 10.2 AAF adducts, 11.5 bulky UV lesions, 5.0 or 16.7 B[*a*]P adducts, and undamaged plasmids pUC19 were prepared as described (20). To obtain competitor DNA with 16.6 platinum cross-links per plasmid, pUC19 DNA (16 nM) was incubated with *cis*-$Pt(NH_3)_2Cl_2$ (5.4 μM) in 10 mM Tris-HCl (pH 8.0) and 1 mM EDTA for 24 h at 37°C. Competitor DNA containing 17.2 monofunctional platinum adducts per plasmid was obtained by reacting pUC19 DNA (16 nM) with [Pt(dien)Cl]Cl (4.3 μM). The extent of platinum modification was determined by atomic absorption spectroscopy (Elan 5000; Perkin-Elmer). CPDs were removed by photoreactivation using *Anacystis nidulans* photolyase and irradiation at 366 nm (21). The efficacy of photoreactivation was confirmed by incubating the plasmids with T4 endonuclease V (22).

Cell-free Extracts and Repair Assays. Extracts were prepared from HeLa cells (23). Repair reactions (50 μl) were performed with 80 μg of cell extract proteins, M13 DNA substrate (0.2 nM), and competitor pUC19 DNA as reported (20). After repair at 30°C for 3 h, reactions were stopped by the addition of EDTA, and the samples were processed by incubation with RNase A and proteinase K. DNA was extracted, digested with *Ava*II, *Pst*I, and *Sma*I, resolved on 20% native polyacrylamide gels, and [^{32}P]dCMP incorporation was visualized by autoradiography followed by laser scanning quantification. Alternatively, repair assays in human cell extracts were performed for 3 h with plasmids pSPORT (2 nM) and pUC19 (3 nM), as indicated in the legend to Fig. 3*C*. To measure DNA repair synthesis, both plasmids were recovered and analyzed as outlined before except that DNA was linearized by *BamH*I and separated on 1% agarose gels. The oligonucleotide excision assay of Fig. 4 was performed by incubating internally labeled substrates (0.2 nM) in cell extract (19). Competitor fragments were added at a concentration of up to 1.8 nM. Excision products were separated on 10% denaturing polyacrylamide gels and visualized by autoradiography.

Received 1/31/02; accepted 5/31/02.

The costs of publication of this article were defrayed in part by the payment of page charges. This article must therefore be hereby marked *advertisement* in accordance with 18 U.S.C. Section 1734 solely to indicate this fact.

[1] Supported by grants from the Swiss National Science Foundation (Grant 31-61494.00), the Krebsliga of the Kanton Zürich, and the NIH (Grant CA 76660).

[2] To whom requests for reprints should be addressed, at Institute of Pharmacology and Toxicology, University of Zürich-Tierspital, August Forel-Strasse 1, CH-8008 Zürich, Switzerland. Phone: 41-1-635-87-63; Fax: 41-1-635-89-10; E-mail: naegelih@vetpharm.unizh.ch.

[3] The abbreviations used are: NER, nucleotide excision repair; AAF, acetylaminofluorene; B[*a*]P, benzo[*a*]pyrene; CPD, cyclobutane pyrimidine dimer.

Analysis of M13/pUC19 Competition Assays. The relative affinity of the NER complex for different adducts was determined from the molar excess of damaged pUC19 DNA, at which repair of the M13 substrate is reduced to 50%, multiplied by the number of lesions per pUC19 molecule. For example, pUC19 DNA containing both CPDs and (6-4) photoproducts (a total of 11.5 bulky UV lesions per plasmid) was able to immobilize NER complexes 2.5 times less efficiently than a single AAF adduct, yielding a relative affinity that was $2.5 \times 11.5 = 29$ times lower for UV lesions compared with the AAF standard. To calculate the relative affinity of NER factors for CPDs (Aff_{CPD}), the following equation was used:

$$11.5 \times \frac{1}{29} = 8.6 \times Aff_{CPD} + 2.9 \times \frac{1}{10}; \; Aff_{CPD} = \frac{1}{80}.$$

where $Aff_{UV} = 1/29$ is the relative affinity of NER factors for the mixture of all of the bulky UV lesions, including CPDs and (6-4) photoproducts, and $Aff_{(6\text{-}4)} = 1/10$ is the relative affinity for (6-4) photoproducts.

RESULTS

Immobilization of NER Factors during Repair of Bulky Lesions. We developed a repair competition assay to analyze the distribution of human NER complexes between multiple forms of damage (Fig. 1*A*). This assay requires substrate DNA, a source of human NER enzymes and competitor DNA. M13 double-stranded DNA containing a single AAF-C^8-dG adduct was used as the NER substrate (Fig. 1*A*). To allow for quantitative analysis of repair reactions, this AAF lesion was flanked by restriction sequences for *Sma*I (23 nucleotides away from the adduct in the 5′ direction) and *Pst*I (13 nucleotides away from the adduct in the 3′ direction). The site-specific substrate was incubated in a standard human cell extract that contains the entire repertoire of NER factors (24, 25). After incubations of 3 h, DNA repair synthesis was monitored by measuring the incorporation of ^{32}P-labeled deoxyribonucleotides in the region of the substrate where the AAF adduct was located before excision, *i.e.*, in the 37-bp *Sma*I-*Pst*I fragment of M13 DNA (Fig. 1*B*, *Lanes 3* and *4*). No DNA repair synthesis was detected in the *Sma*I-*Pst*I region of undamaged M13 DNA (*Lanes 1 and 2*).

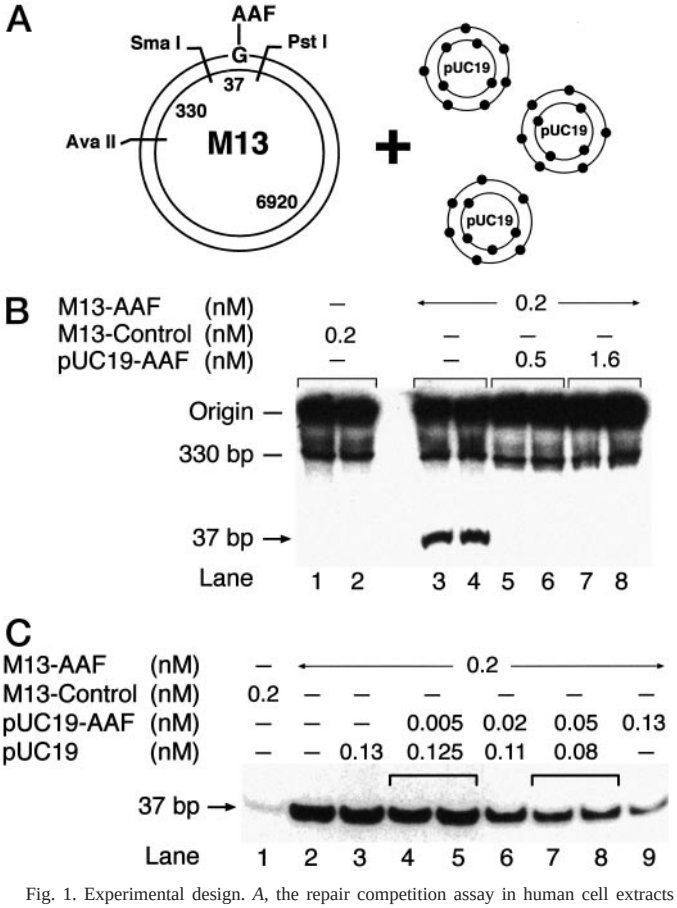

Fig. 1. Experimental design. *A*, the repair competition assay in human cell extracts determines the capacity of DNA lesions located on plasmids pUC19 to immobilize human NER factors and, hence, compete for repair of the single AAF adduct located on M13 substrate. *B*, damage-specific [^{32}P]dCMP incorporation in the 37-bp *Sma*I-*Pst*I region of M13 DNA, accompanied by nonspecific incorporation in the long *Pst*I-*Ava*II fragment (migrating near the origin) and the *Ava*II-*Sma*I fragment (330 bp). *Lanes 1* and *2*, incubations with undamaged M13 substrate; *Lanes 5–8*, complete inhibition of substrate repair by adding AAF-damaged pUC19 DNA. *C*, dose-dependent inhibition of substrate repair by adding increasing concentrations of AAF-damaged pUC19 competitor. Only [^{32}P]dCMP incorporation in the 37-bp *Sma*I-*Pst*I region is shown. *Lane 1*, control reaction with undamaged M13 substrate.

We combined M13 DNA containing the single AAF adduct with pUC19 DNA containing, on the average, 10.2 AAF adducts per molecule. When this mixture was incubated for 3 h in cell extract, repair patch synthesis in the 37-bp *Sma*I-*Pst*I region of the substrate was suppressed (Fig. 1*B*, *Lanes 5–8*). In dose response experiments, 50% inhibition of substrate repair was detected by adding AAF-damaged pUC19 DNA at a concentration of 0.02 nM, corresponding to a 10-fold molar excess of M13 substrate over pUC19 competitor (Fig. 1*C*, *Lane 6*). Because each M13 DNA molecule carried only one AAF adduct, whereas pUC19 DNA contained on the average 10.2 adducts, these results showed that 50% inhibition of substrate repair is observed when there is a 1:1 distribution of DNA lesions between substrate and competitor DNA. Thus, the single site-directed AAF lesion in M13 substrate immobilizes NER factors as efficiently as the multiple AAF modifications located on pUC19 competitor. No reduction of substrate repair was observed when the reactions were incubated with undamaged pUC19 DNA (Fig. 1*C*, *Lane 3*).

Validation of the Immobilization Assay. A comparison between base adducts of either cisplatin or a monofunctional platinum analogue confirmed that immobilization of NER proteins is strictly dependent on the ability of the NER complex to recognize a competitor lesion. Exposure of DNA to *cis*-$Pt(NH_3)_2Cl_2$ (cisplatin) results in the formation of 1,2-intrastrand platinum cross-links between the N^7 positions of purine bases, accompanied by minor fractions of 1,3-intrastrand cross-links and interstrand cross-links (26). In contrast, the [Pt(dien)Cl]Cl analogue is unable to cross-link the bases and generates only monofunctional adducts at N^7 of guanine (16). Plasmids pUC19 with ~17 covalent modifications per molecule, either cross-links or monoadducts, were tested in the repair competition assay. We found nearly 50% inhibition of substrate repair in the presence of an 8-fold molar excess of cisplatin-damaged pUC19 over M13 DNA (Fig. 2*A*, *Lanes 4 and 5*), but a stronger inhibition was induced with a 25-fold excess of cisplatin-damaged competitor (Fig. 2*A*, *Lanes 8 and 9*). In contrast to cisplatin cross-links, monofunctional Pt(dien) adducts were essentially unable to immobilize NER factors such that repair of the AAF substrate was not reduced even when Pt(dien)-modified pUC19 was added in a 25-fold excess over M13 DNA (Fig. 2*B*, *Lanes 7* and *8*).

The relative immobilization of NER factors because of a particular lesion was determined from the molar excess of damaged pUC19 DNA at which repair of the M13 substrate is reduced to 50%, multiplied by the number of adducts per pUC19 molecule (Fig. 2*C*). Considering that half-maximal inhibition was detected at an 8-fold molar excess of cisplatin-damaged pUC19 DNA and that each pUC19 molecule contained, on the average, 16.7 cisplatin modifications, these results indicate that cisplatin cross-links immobilize NER factors $8 \times 16.7 = 134$ times less efficiently than AAF adducts. For comparison, we tested pUC19 plasmids containing DNA adducts generated by diol epoxide derivatives of B[*a*]P, a widespread envi-

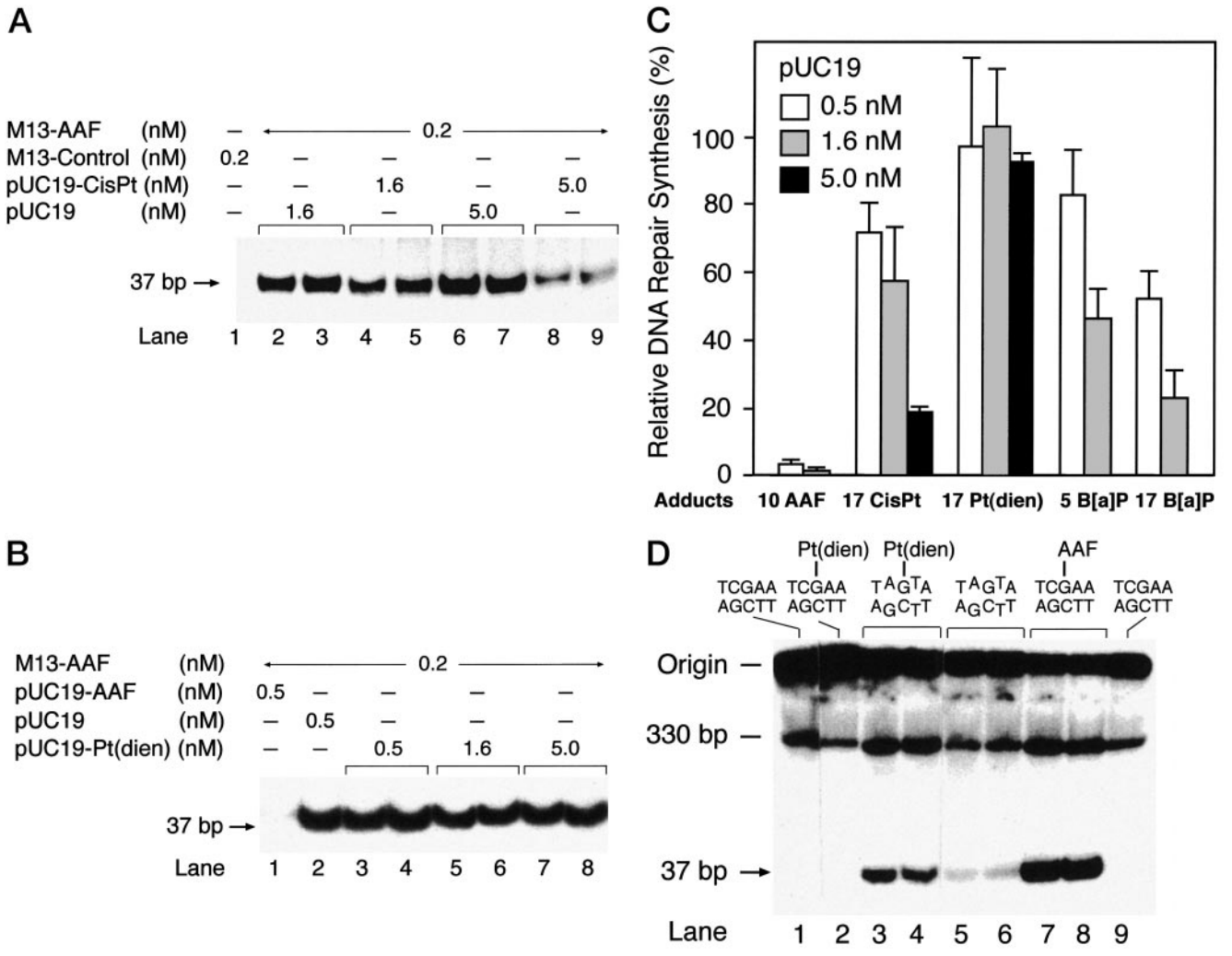

Fig. 2. Immobilization of NER factors during excision of bulky lesions. *A*, dose-dependent inhibition of M13 substrate repair by addition of cisplatin-damaged pUC19 DNA. *B*, failure of Pt(dien)-damaged DNA to compete with repair of the M13 substrate. *Lane 1*, control reaction containing AAF-damaged pUC19 competitor. *C*, summary plot showing the inhibition of M13 substrate repair because of various types of competitor pUC19 DNA at concentrations between 0.5 and 5.0 nM. The number of adducts per pUC19 molecule is indicated. *D*, in contrast to AAF adducts (*Lanes 7* and *8*), Pt(dien) adducts are not excised from M13 double-stranded DNA (*Lane 2*). In the substrates of *Lanes 3* and *4*, the single Pt(dien) adduct was combined with base mismatches to increase local distortion; *bars*, ±SD.

ronmental contaminant (Fig. 2*C*). Repair of the AAF substrate was reduced to 50% when pUC19 plasmids with 5.0 B[*a*]P adducts per molecule were added in an 8-fold molar excess (Fig. 2*C*). This ratio translates to a $5.0 \times 8 = 40$-fold preference of NER factors for AAF adducts compared with B[a]P adducts. After increasing the B[*a*]P adducts from 5.0 to 16.6 per pUC19 molecule, repair of the AAF substrate was already inhibited to 50% when B[*a*]P-damaged competitor was added in a 2.5-fold excess. This ratio indicates a $16.6 \times 2.5 = 42$-fold preference for AAF adducts compared with B[*a*]P adducts. Thus, the repair competition assay yields the same relative affinity of NER factors for a particular lesion, independently of the frequency of pUC19 modification. Consistent with previous observations (27), a single Pt(dien)-dG monoadduct in the *Sma*I-*Pst*I region of M13 DNA induced DNA repair synthesis only when the platinum lesion was combined with base mismatches that enhance local helical distortion (Fig. 2*D*, compare *Lane 2* with *Lanes 3* and *4*). Thus, the human NER system fails to process a monofunctional platinum adduct in duplex DNA and this finding correlates with the failure of Pt(dien)-modified pUC19 plasmids to immobilize NER factors in the competition assay. We concluded that the repair competition assay provides a quantitative tool to monitor the immobilization of human NER proteins during their involvement in bulky lesion repair.

Distribution of Repair Activity between AAF Adducts and UV Radiation Products. We exploited the repair competition assay to examine the interaction of human NER factors with mixtures of bulky adducts. For that purpose, the M13 substrate carrying the single AAF adduct was incubated with increasing amounts of pUC19 DNA that contained 11.5 bulky UV lesions per plasmid (Fig. 3*A*). Half-maximal inhibition of substrate repair was found when UV-damaged pUC19 DNA was added in a 2.5-fold molar excess (Fig. 3*B*), indicating that UV photoproducts immobilize human NER factors $2.5 \times 11.5 = 29$ times less efficiently than AAF adducts. This evaluation is complicated by the fact that UV-C irradiation induces CPDs and (6-4) photoproducts in a ratio of 3: 1 (12). Thus, the UV-irradiated pUC19 competitor DNA contained, on the average, ~9 CPDs and 3 (6-4) photoproducts per molecule. To determine the contribution of each photoproduct, the plasmids were photoreactivated to remove CPDs and generate pUC19 competitor DNA with only (6-4) photoproducts. However, the inhibitory effect of UV-irradiated plasmids was only marginally diminished after complete removal of CPDs (Fig. 3, *A* and *B*), indicating that (6-4) photoproducts, and not CPDs, are mainly

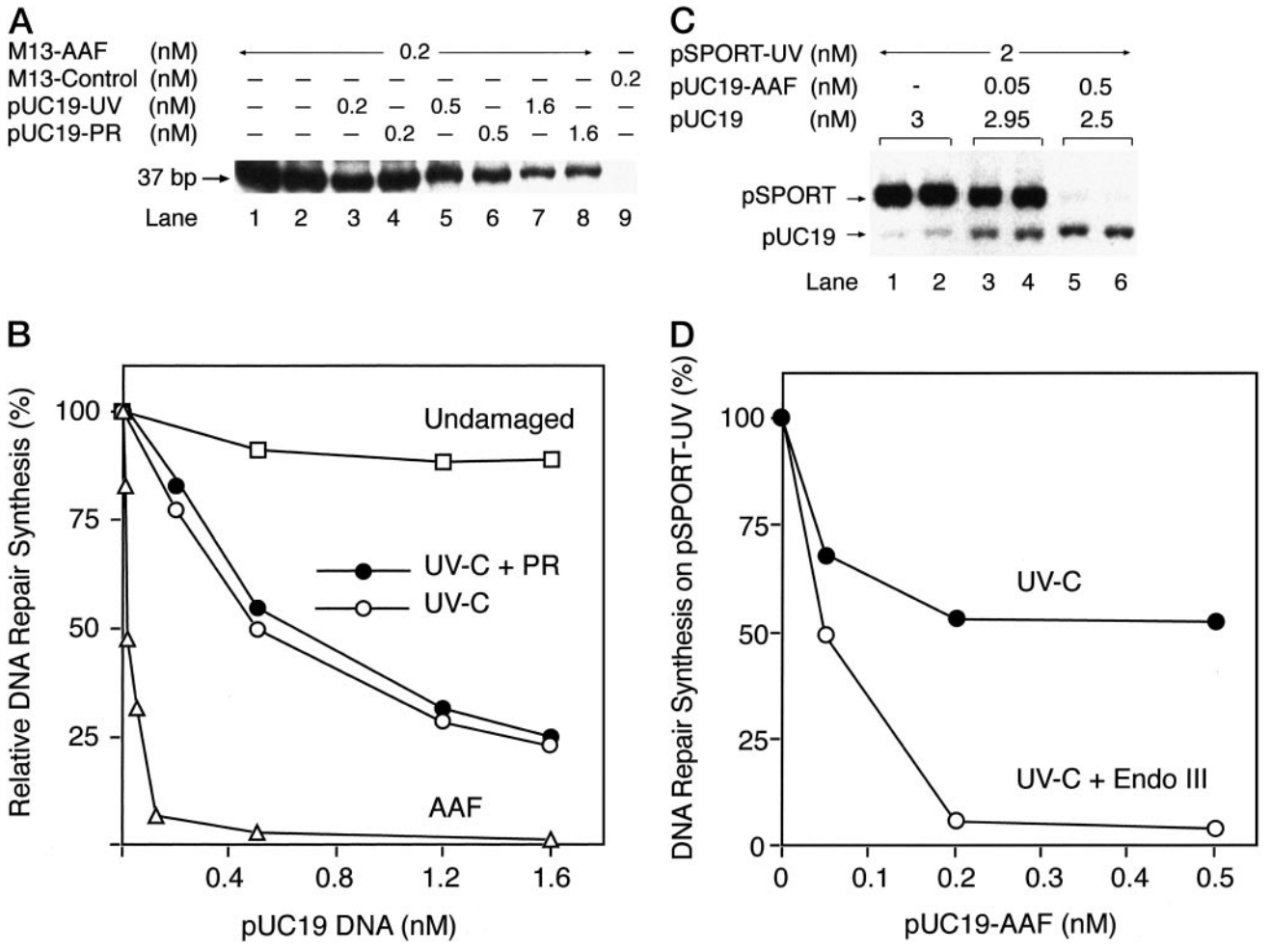

Fig. 3. Distribution of repair activity between AAF adducts and UV photoproducts. *A*, inhibition of M13 substrate repair by addition of UV-irradiated pUC19 competitor; *pUC19-PR*, plasmids pUC19 were photoreactivated to remove all of the CPDs (*Lanes 4*, *6*, and *8*). *B*, quantification of two independent experiments, showing that (6-4) photoproducts (obtained by photoreactivation of UV-irradiated pUC19) are responsible for the immobilization of NER factors. *C*, AAF-damaged pUC19 DNA antagonizes the repair of UV-irradiated DNA (*Lanes 5* and *6*). UV-irradiated pSPORT (2 nM) and plasmids pUC19 (3 nM) were coincubated in cell extract in the presence of [^{32}P]dCTP. Base excision repair substrates were excluded from pSPORT by treatment with endonuclease III followed by removal of nicked DNA. *D*, quantification of two independent experiments, showing that AAF-damaged competitor is able to reduce repair patch synthesis in UV-irradiated plasmid pSPORT. The pSPORT substrates were tested directly or after pretreatment with endonuclease III.

responsible for the immobilization of NER factors. By interpolation of the data plotted in Fig. 3*B*, we found that a 3.4-fold excess of photoreactivated pUC19, containing 3 (6-4) photoproducts, was required to obtain 50% inhibition of AAF substrate repair. These numbers translate to a $3.4 \times 3 = 10$-fold higher affinity for AAF adducts relative to (6-4) photoproducts. Additional calculations indicated that CPDs immobilize NER factors 80 times less efficiently than AAF adducts (see "Materials and Methods").

The strong bias of human NER factors for AAF-damaged DNA implied that the presence of AAF adducts could suppress the concomitant repair of UV lesions added to the same reaction mixture. To test this prediction, UV-irradiated (450 J/m^2) and endonuclease III-treated plasmid pSPORT was coincubated in cell extract with pUC19 DNA. Excision of UV photolesions was determined by monitoring repair patch synthesis in the presence of ^{32}P-labeled dCTP. As expected, the repair of UV-irradiated pSPORT DNA was progressively inhibited by adding AAF-damaged pUC19 DNA (Fig. 3*C*, *Lanes 3–6*). Interestingly, the loss of repair patches in UV-irradiated pSPORT was only partially compensated by a concurrent increase of DNA repair synthesis on pUC19 (compare Fig. 3*C*, *Lanes 1* and *2* with *Lanes 5* and *6*). Pretreatment with endonuclease III (followed by purification of closed circular DNA) is required to eliminate plasmids that contain pyrimidine hydrates. When these base excision repair substrates were left in pSPORT, the repair of UV radiation products was only partially inhibited by the addition of AAF-damaged pUC19 DNA (Fig. 3*D*). Thus, the reduction of repair activity is because of immobilization of NER subunits, whereas other factors, in particular those involved in base excision repair, are not immobilized by AAF adducts.

Construction of a Prototype Decoy DNA Adduct. Our results indicated that some AAF lesions exert an antagonistic activity on DNA repair without inducing any excision. This finding led us to search for DNA damage that, like the AAF adduct, is able to immobilize NER factors but, unlike the AAF adduct, is not amenable to excision. To construct such a prototype decoy lesion, we manipulated the nucleotide sequence environment at the site of damage. First, we noted that excision of AAF-dG adducts from DNA duplexes of 139 bp was reduced ~10-fold when the dCMP residue located in the nondamaged strand opposite the modified guanine was removed (data not shown). This inhibition was even more pronounced when we performed the same experiment with B[*a*]P adducts. In cell extract, excision of the (+)-*trans-anti*-B[*a*]P-dG adduct (as a component of 24–32-nucleotides long products) was marginally affected when the cytosine opposite the damaged guanine was replaced by adenine (Fig. 4*A*, compare *Lanes 4* and *5*). In contrast, excision of the same (+)-*trans-anti*-B[*a*]P-dG adduct was abolished when the dCMP res-

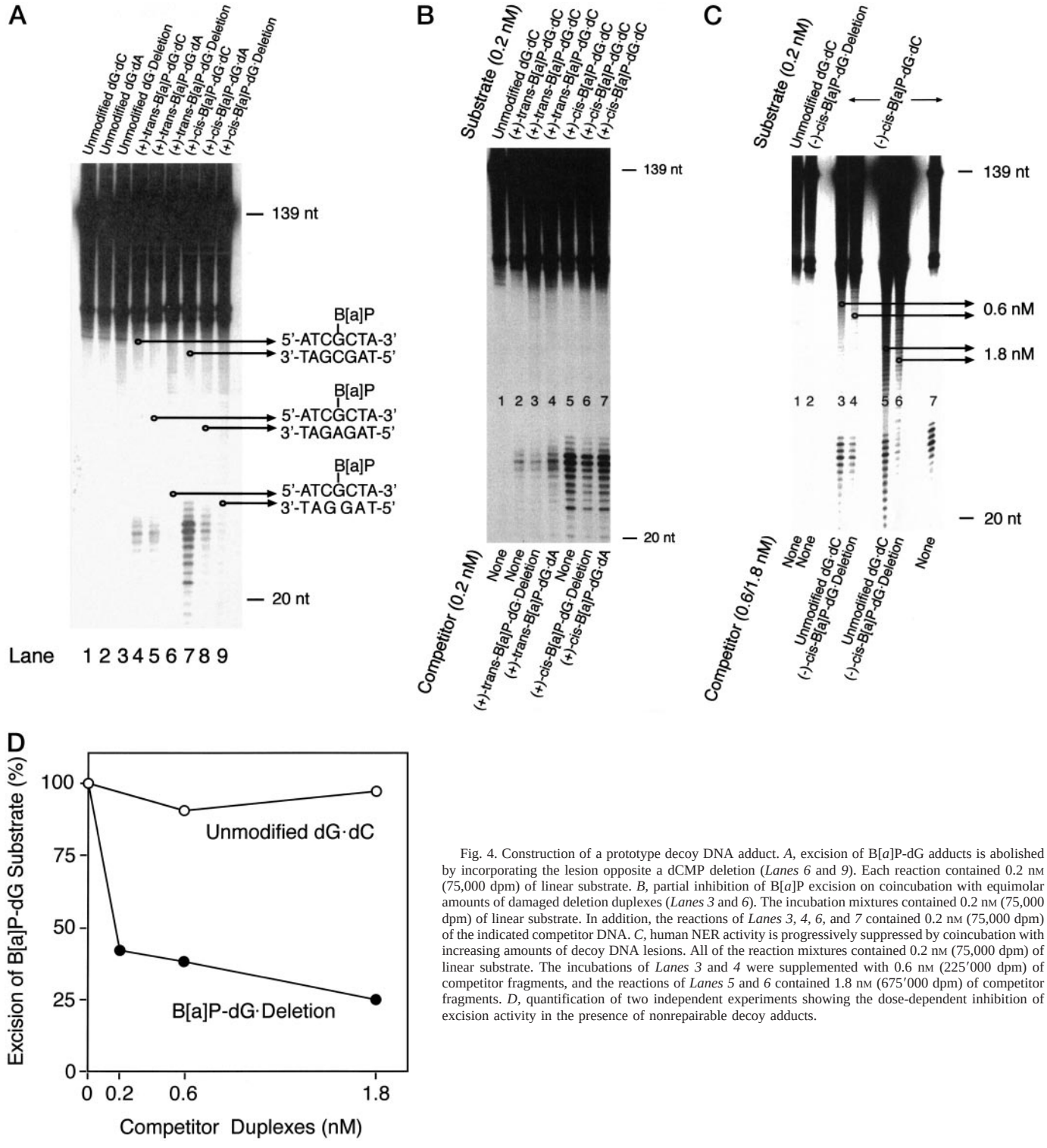

Fig. 4. Construction of a prototype decoy DNA adduct. *A*, excision of B[*a*]P-dG adducts is abolished by incorporating the lesion opposite a dCMP deletion (*Lanes 6* and *9*). Each reaction contained 0.2 nM (75,000 dpm) of linear substrate. *B*, partial inhibition of B[*a*]P excision on coincubation with equimolar amounts of damaged deletion duplexes (*Lanes 3* and *6*). The incubation mixtures contained 0.2 nM (75,000 dpm) of linear substrate. In addition, the reactions of *Lanes 3*, *4*, *6*, and *7* contained 0.2 nM (75,000 dpm) of the indicated competitor DNA. *C*, human NER activity is progressively suppressed by coincubation with increasing amounts of decoy DNA lesions. All of the reaction mixtures contained 0.2 nM (75,000 dpm) of linear substrate. The incubations of *Lanes 3* and *4* were supplemented with 0.6 nM (225′000 dpm) of competitor fragments, and the reactions of *Lanes 5* and *6* contained 1.8 nM (675′000 dpm) of competitor fragments. *D*, quantification of two independent experiments showing the dose-dependent inhibition of excision activity in the presence of nonrepairable decoy adducts.

idue across the lesion was deleted (Fig. 4*A*, *Lane 6*). This observation was extended by exploiting the stereochemistry of B[*a*]P-dG lesions, because the adducts with *cis* configuration are excised more efficiently than the corresponding *trans* isomers (19). Interestingly, excision of the (+)-*cis*-*anti*-B[*a*]P-dG isomer was reduced in the dG·dA context (Fig. 4*A*, compare *Lanes 7* and *8*), and excision of the same (+)-*cis*-*anti*-B[*a*]P-dG adduct was essentially abolished when the dCMP opposite the lesion was deleted (Fig. 4*A*, *Lane 9*).

The conformation of deletion duplexes containing B[*a*]P-N^2-dG lesions has been determined, thereby revealing that these adducts form wedge-shaped intercalation complexes (28, 29). Thus, all of the subsequent studies were performed with these highly defined B[*a*]P adducts instead of the AAF lesion. In particular, the complete lack of excision of adducts from the deletion duplexes allowed us to perform competition experiments in which a site-directed repair substrate was combined with these damaged deletion fragments. In the experiment of Fig. 4*B*, DNA substrates (0.2 nM) containing either a (+)-*trans*-*anti*-B[*a*]P adduct or a (+)-*cis*-*anti*-B[*a*]P adduct were mixed with

equimolar amounts of the respective competitor DNA fragments of identical length. Surprisingly, there was inhibition of repair of the (+)-*trans*-*anti*-B[*a*]P-dG substrates when the competitor DNA carried the same B[*a*]P adduct at a deletion site lacking the cytosine residue opposite the lesion (Fig. 4*B*, compare *Lanes 2 and 3*). This inhibition was not observed when the substrate was coincubated with the same lesion in the dG.dA context used as a competitor (Fig. 4*B*, *Lane 4*). Inhibition of repair was also detected when the (+)-*cis*-*anti*-B[*a*]P-dG substrate was mixed with equimolar amounts of competitor fragments carrying the same adduct opposite a deletion site (Fig. 4*B*, compare *Lanes 5 and 6*). Again, this inhibition was not detected when the substrate was coincubated with the same lesion in the dG·dA context as a competitor (Fig. 4*B*, *Lane 7*). Additional control experiments showed that deletion sites alone, in the absence of covalent B[*a*]P modifications, failed to inhibit excision repair activity (data not shown). Finally, internally radiolabeled substrates containing a site-specific (−)-*cis*-*anti*-B[*a*]P adduct were used to establish the dose response shown in Fig. 4*C*. The addition of deletion duplexes containing the same (−)-*cis*-*anti*-B[*a*]P-dG adduct, but with a missing dCMP residue, in a 3-fold (Fig. 4*C*, *Lane 4*) or 9-fold molar excess (Fig. 4*C*, *Lane 6*) resulted in progressive inhibition of substrate repair. However, excision was only marginally reduced when the same amounts of unmodified duplexes were added to the assay mixtures (Fig. 4*C*, *Lanes 3 and 5*). A quantitative evaluation of substrate repair as a function of competitor concentrations is shown in Fig. 4*D*. These results demonstrate that human NER factors are susceptible to hijacking by specific decoy adducts.

DISCUSSION

Previous studies showed that the NER complex removes DNA adducts with vastly different efficiencies. In UV-irradiated human cells, for example, (6-4) photoproducts are repaired rapidly with 50% excision after 2 h or less, whereas CPDs are removed with a half-life of ~8 h (12–14). Repair half-lives in the range of 2 h were also detected by monitoring the removal of AAF-dG adducts from human genomic DNA (30). A comparable relationship resulted from reactions performed in a human cell extract that excludes possible interferences because of chromatin assembly or transcriptional activity. These *in vitro* reactions confirmed that (6-4) photoproducts and AAF adducts are processed by human NER enzymes with similar efficiency, whereas excision of CPDs was promoted at slower rates (31). Thus, we used the same cell extract to compare the affinity of human NER factors for a series of bulky DNA adducts. Coincubation of different standard NER substrates in the same reaction mixture demonstrated that a single site-directed AAF adduct competes for a limited pool of human NER factors ~10 times more efficiently than (6-4) photoproducts and nearly 100 times more efficiently than CPDs. This discrepancy between the recruitment of NER factors, where the AAF adduct is 10-fold more effective than (6-4) photoproducts, and the corresponding excision rates, with no significant difference between the two lesions, indicated that some AAF adducts cause immobilization of repair proteins instead of excision of the offending lesion. The notion that a fraction of carcinogen adducts may exert an antagonistic activity on DNA repair was supported by two subsequent experiments. First, the addition of AAF-damaged DNA suppressed the concomitant repair of UV-irradiated DNA, confirming that a subset of AAF adducts negatively regulates human NER activity. Second, we were able to construct a prototype decoy adduct that retains the ability to compete for NER activity but is completely refractory to excision.

The rational basis for engineering such a decoy lesion was prompted by the conformational variability of many carcinogen-damaged sites, including the AAF-C^8-dG lesion and several B[*a*]P-N^2-dG adducts (32–34). This polymorphism suggested that the various local structure may determine whether damage recognition is followed by excision or, alternatively, by immobilization of NER proteins without excision. To test this hypothesis, the double helical conformation at the site of covalent binding was manipulated by altering the local base composition. Surprisingly, we found that deletion of the dCMP residue opposite the tested B[*a*]P-dG adducts not only abolished excision but also conferred the ability to compete with repair of normal substrates added to the same reactions. Apparently, this dCMP deletion stabilized an adduct conformation that is endowed with the expected properties of a decoy lesion.

The prototype decoy adduct consisting of a bulky lesion opposite dCMP deletions has been identified as a mutagenic intermediate after the replicative bypass of AAF or B[*a*]P adducts. In fact, translesion synthesis across these adducts is facilitated by a mechanism in which one strand can slip with respect to the other strand, generating misalignment frameshifts in the daughter strand. Depending on the sequence context, single nucleotide deletions across the adduct constitute the predominant source of carcinogen-induced mutations (35–37). Such single nucleotide deletions have also been found in the chromosomal hypoxanthine phosphoribosyltransferase gene after exposing human cells to B[*a*]P diol epoxides (38). Thus, the type of decoy lesion identified in the present study is normally generated in many cases of environmental genotoxic stress. Furthermore, the discovery of such a prototype decoy adduct shows that human NER subunits are susceptible to hijacking and, hence, raises the possibility that particular fractions of genotoxic mixtures may induce bulky DNA lesions that exert negative effects on DNA repair. The resulting antagonism between substrate and decoy adducts could be responsible for hyperadditive interactions between multiple genotoxic agents.

Trapping of nucleotide excision repair factors by nonrepairable decoy DNA adducts is a new genotoxic reaction that has not been described before. Previously, Treiber *et al.* (39) and McLeod *et al.* (40) reported that certain transcription factors may bind to cisplatin cross-links or B[*a*]P adducts, thus protecting these lesions from DNA repair processes. Another study showed that poly(ADP-ribose) polymerase may obstruct DNA repair by interacting with DNA ends (41). Thus, the concept of protein hijacking was introduced to indicate that specific DNA lesions elicit toxic responses through sequestration of essential transcription factors (39, 40). The present study rules out any participation of transcription factors or other chromatin components and reveals a novel mechanism of repair inhibition because of direct immobilization of NER factors. As a consequence, excision complexes are titrated away from their sites of action on substrates that are normally susceptible to DNA repair.

REFERENCES

1. Friedberg, E. C., Walker, G. C., and Siede, W. DNA Repair and Mutagenesis. Washington, DC: American Society of Microbiology, 1995.
2. Sancar, A. DNA excision repair. Annu. Rev. Biochem., *65:* 43–81, 1996.
3. Lindahl, T., and Wood, R. D. Quality control by DNA repair. Science (Wash. DC), *286:* 1897–1905, 1999.
4. de Boer, J., and Hoeijmakers, J. H. Nucleotide excision repair and human syndromes. Carcinogenesis (Lond.), *21:* 453–460, 2000.
5. Huang, J-C., Svoboda, D. L., Reardon, J. T., and Sancar, A. Human nucleotide excision nuclease removes thymine mimers from DNA by incising the 22nd phosphodiester bond 5′ and the 6th phosphodiester bond 3′ to the photodimer. Proc. Natl. Acad. Sci. USA, *89:* 3664–3668, 1992.
6. Shivji, M. K., Podust, V. N., Hübscher, U., and Wood, R. D. Nucleotide excision repair DNA synthesis by DNA polymerase ϵ in the presence of PCNA, RFC, and RPA. Biochemistry, *34:* 5011–5017, 1995.
7. Sancar, A., and Rupp, W. D. A novel repair enzyme: UVRABC excision nuclease of *Escherichia coli* cuts a DNA strand on both sides of the damaged region. Cell, *33:* 249–260, 1983.
8. Guzder, S. N., Habraken, Y., Sung, P., Prakash, L., and Prakash, S. Reconstitution of yeast nucleotide excision repair with purified Rad proteins, replication protein A, and transcription factor TFIIH. J. Biol. Chem., *270:* 12973–12976, 1995.

9. Aboussekhra, A., Biggerstaff, M., Shivji, M. K., Vilpo, J. A., Moncollin, V., Podust, V. N., Protic, M., Hübscher, U., Egly, J-M., and Wood, R. D. Mammalian DNA nucleotide excision repair reconstituted with purified components. Cell, *80:* 859–868, 1995.
10. Mu, D., Park, C-H., Matsunaga, T., Hsu, D. S., Reardon, J. T., and Sancar, A. Reconstitution of human DNA repair excision nuclease in a highly defined system. J. Biol. Chem., *270:* 2415–2418, 1995.
11. Araujo, S. J., Tirode, F., Coin, F., Pospiech, H., Syväoja, J. E., Stucki, M., Hübscher, U., Egly, J-M., and Wood, R. D. Nucleotide excision repair of DNA with recombinant human proteins: definition of the minimal set of factors, active forms of TFIIH, and modulation by CAK. Genes Dev., *14:* 349–359, 2000.
12. Mitchell, D. L. The relative cytotoxicity of (6-4) photoproducts and cyclobutane dimers in mammalian cells. Photochem. Photobiol., *48:* 51–57, 1988.
13. Vreeswijk, M. P., van Hoffen, A., Westland, B. E., Vrieling, H., van Zeeland, A. A., and Mullenders, L. H. Analysis of repair of cyclobutane pyrimidine dimers and pyrimidine 6-4 pyrimidone photoproducts in transcriptionally active and inactive genes in Chinese hamster cells. J. Biol. Chem., *269:* 31858–31863, 1994.
14. Ford, J. M., and Hanawalt, P. C. Expression of wild-type p53 is required for efficient global genomic nucleotide excision repair in UV-irradiated human fibroblasts. J. Biol. Chem., *272:* 28073–28080, 1997.
15. Hansson, J., Munn, M., Rupp, W. D., Kahn, R., and Wood, R. D. Localization of DNA repair synthesis by human cell extracts to a short region at the site of a lesion. J. Biol. Chem., *264:* 21788–21792, 1989.
16. Johnson, N. P., Macquet, J. P., Wiebers, J. L., and Monsarrat, B. Structures of the adducts formed between [Pt(dien)Cl]Cl and DNA *in vitro*. Nucleic Acids Res., *10:* 5255–5271, 1982.
17. Hess, M. T., Gunz, D., and Naegeli, H. A repair competition assay to assess recognition by human nucleotide excision repair. Nucleic Acids Res., *24:* 824–828, 1996.
18. Biggerstaff, M., Robins, P., Coverley, D., and Wood, R. D. Effect of exogenous DNA fragments on human cell extract-mediated DNA repair synthesis. Mutat. Res., *254:* 217–224, 1991.
19. Hess, M. T., Gunz, D., Luneva, N., Geacintov, N. E., and Naegeli, H. Base pair conformation-dependent excision of benzo[*a*]pyrene diol epoxide-guanine adducts by human nucleotide excision repair enzymes. Mol. Cell. Biol., *17:* 7069–7076, 1997.
20. Gunz, D., Hess, M. T., and Naegeli, H. Recognition of DNA adducts by human nucleotide excision repair. J. Biol. Chem., *271:* 25089–25098, 1996.
21. Eveno, E., Bourre, F., Quillet, X., Chevallier-Lagente, O., Roza, L., Eker, A. P., Kleijer, W. J., Nikaido, O., Stefanini, M., and Hoeijmakers, J. H. Different removal of ultraviolet photoproducts in genetically related xeroderma pigmentosum and trichothiodystrophy diseases. Cancer Res., *55:* 4325–4332, 1995.
22. Jones, C. J., and Wood, R. Preferential binding of the xeroderma pigmentosum group A complementing protein to damaged DNA. Biochemistry, *32:* 12096–12104, 1993.
23. Manley, J. L., Fire, A., Cano, A., Sharp, P. A., and Gefter, M. L. DNA-dependent transcription of adenovirus genes in a soluble whole-cell extract. Proc. Natl. Acad. Sci. USA, *77:* 3855–3859, 1980.
24. Wood, R. D., Robins, P., and Lindahl, T. Complementation of the xeroderma pigmentosum DNA repair defect in cell-free extracts. Cell, *53:* 97–106, 1988.
25. Sibghat-Ullah, Husain, I., Carlton, W., and Sancar, A. Human nucleotide excision repair *in vitro*: repair of pyrimidine dimers, psoralen and cisplatin adducts by HeLa cell-free extract. Nucleic Acids Res., *17:* 4471–4484, 1989.
26. Pinto, A. L., and Lippard, S. J. Binding of the antitumor drug *cis*-diamminedichloroplatinum(II) (cisplatin) to DNA. Biochim. Biophys. Acta, *780:* 167–180, 1985.
27. Calsou, P., Frit, P., and Salles, B. Repair synthesis by human cell extracts in cisplatin-damaged DNA is preferentially determined by minor adducts. Nucleic Acids Res., *20:* 6363–6368, 1992.
28. Cosman, M., Fiala, R., Hingerty, B. E., Amin, S., Geacintov, N. E., Broyde, S., and Patel, D. J. Solution conformation of the (+)-*trans-anti*-[BP]dG adduct opposite a deletion site in a DNA duplex: intercalation of the covalently attached benzo[*a*]pyrene into the helix with base displacement of the modified deoxyguanosine into the major groove. Biochemistry, *33:* 11507–11517, 1994.
29. Cosman, M., Fiala, R., Hingerty, B. E., Amin, S., Geacintov, N. E., Broyde, S., and Patel, D. J. Solution conformation of the (+)-*cis-anti*-[BP]dG adduct opposite a deletion site in a DNA duplex: intercalation of the covalently attached benzo[*a*]pyrene into the helix with base displacement of the modified deoxyguanosine into the minor groove. Biochemistry, *33:* 11518–11527, 1994.
30. van Oostervijk, M. F., Filon, R., de Groot, A. J., van Zeeland, A. A., and Mullenders, L. H. Lack of transcription-coupled repair of acetylaminofluorene DNA adducts in human fibroblasts contrasts their efficient inhibition of transcription. J. Biol. Chem., *273:* 13599–13604, 1998.
31. Szymkowski, D. E., Lawrence, C. W., and Wood, R. D. Repair by human cell extracts of single (6-4) and cyclobutane thymine-thymine photoproducts in DNA. Proc. Natl. Acad. Sci. USA, *90:* 9823–9827, 1993.
32. Veaute, X., and Fuchs, R. P. Polymorphism in *N*-2-acetylaminofluorene-induced DNA structure as revealed by DNase I footprinting. Nucleic Acids Res., *19:* 5603–5606, 1991.
33. Mu, D., Bertrand-Burggraf, E., Huang, J. C., Fuchs, B. P., Sancar, A., and Fuchs, R. P. Human and *E. coli* excinucleases are affected differently by the sequence context of acetylaminofluorene-guanine adduct. Nucleic Acids Res., *22:* 4869–4871, 1994.
34. Geacintov, N. E., Cosman, M., Hingerty, B. E., Amin, S., Broyde, S., and Patel, D. J. NMR solution structures of stereoisomeric covalent polycyclic aromatic carcinogen-DNA adducts: principles, patterns, and diversity. Chem. Res. Toxicol., *10:* 111–146, 1997.
35. Koffel-Schwartz, N., Verdier, J. M., Bichara, M., Freund, A. M., Daune, M. P., and Fuchs, R. P. Carcinogen-induced mutation spectrum in wild-type, uvrA and umuC strains of *Escherichia coli.* Strain specificity and mutation-prone sequences. J. Mol. Biol., *177:* 35–51, 1984.
36. Shibutani, S., Margulis, A., Geacintov, N. E., and Grollman, A. P. Translesional synthesis on a DNA template containing a single stereoisomer of dG-(+)- or dG-(-)-*anti*-BPDE (7,8-dihydroxy-anti-9,10-epoxy-7,8,9,10-tetrahydrobenzo[*a*]pyrene). Biochemistry, *32:* 7531–7541, 1993.
37. Moriya, M., Spiegel, S., Fernandes, A., Amin, S., Liu, T., Geacintov, N. E., and Grollman, A. P. Fidelity of translesional synthesis past benzo[*a*]pyrene diol epoxide-2′-deoxyguanosine DNA adducts: marked effects of host cell, sequence context, and chirality. Biochemistry, *35:* 16646–16651, 1996.
38. Chen, R-H., Maher, V. M., and McCormick, J. J. Effect of excision repair by diploid human fibroblasts on the kinds and locations of mutations induced by (±)-7β,8α-dihydroxy-9α,10α-epoxy-7,8,9,10-tetrahydrobenzo[*a*]pyrene in the coding region of the *HPRT* gene. Proc. Natl. Acad. Sci. USA, *87:* 8680–8684, 1990.
39. Treiber, D. K., Zhai, X., Jantzen, H-M., and Essigmann, J. M. Cisplatin-DNA adducts are molecular decoys for the ribosomal RNA transcription factor hUBF (human upstream binding factor). Proc. Natl. Acad. Sci. USA, *91:* 5672–5676, 1994.
40. McLeod, M. C., Powell, K. L., and Tran, N. Binding of the transcription factor, Sp1, to non-target sites in DNA modified by benzo[*a*]pyrene diol epoxide. Carcinogenesis (Lond.), *16:* 975–983, 1995.
41. Satoh, M. S., Poirier, G. G., and Lindahl, T. Dual function for poly(ADP-ribose) synthesis in response to DNA strand breakage. Biochemistry, *33:* 7099–7106, 1994.